Article

Journal of
Nanoscience and Nanotechnology
Vol. 14, 2799–2809, 2014
www.aspbs.com/jnn

Zr Mesoporous Molecular Sieves as Novel Solid Acid Catalysts in Synthesizing Nitrile and Caprolactam

D. Nedumaran[1,2,3] and A. Pandurangan[1,2,*]

[1] Department of Chemistry, Anna University, Chennai 600025, India
[2] Institute for Catalysis and Petroleum Technology, Anna University, Chennai 600025, India
[3] Department of Chemistry, RMK Engineering College, Chennai 601206, India

Zr mesoporous materials with different Si/Zr ratio were synthesized by the surfactant-templated method involving cetyl trimethyl ammonium bromide (CTAB) as template and tetraethyl ortho silicate (TEOS) as organic source of silicon. The synthesized materials were labeled as SiZrMx (where x is Si/Zr = 10, 20 and 30). The BET analysis showed bimodal distribution of pores in SiZrMx structure. An attempt was made to generate super acidity on SiZrM20 by sulfation using sulfuric acid and ammonium sulfate (wt% = 4, 8 and 12). The NH_3-TPD results revealed the presence of strong acidity in sulfated Zr-MCM-41. To understand the nature of acidity in Sulfated Zr-MCM-41, the efficiency of the materials is investigated in dehydration of Oximes. The industrially important materials caprolactam and intermediate nitrile were synthesized from their oximes in liquid phase system. Due to strong acidity in sulfated Zr-MCM-41, fast deactivation was observed during the synthesis of caprolactam but, the catalyst showed 96% nitrile selectivity. The strong acidity and medium strong acidity favoured the formation of nitrile and caprolactam respectively. This study revealed the molecular sieves were effective and eco-friendly solid acid catalysts for synthesizing caprolactam and nitrile.

Keywords: Sulfated Zr-MCM-41, Cyclohexanone Oxime, Caprolactam, Salicylaldoxime, 2-Hydroxy Benzonitrile.

1. INTRODUCTION

In recent years researchers are attracted by mesoporous materials due to its unique physio-chemical properties and potential application in the field of Nanoscience and Nanotechnology. Its tailor made physico-chemical properties like well-defined tunable pore structure, large surface area, ion exchange ability to replace the Si with heteroatom, thermal stability and easy to make up bulk material, it is widely used in catalysis,[1–4] material adsorption,[5–11] biomedical uses such as drug delivery,[12–14] molecular sensing,[15] and advanced applications including fuel/solar cell applications,[16,17] Mesoporous materials can be prepared in various morphologies including powders and films where pore alignment and orientations can also be controlled. These materials are produced by using template syntheses of self-assembled micelle structures and low-cost material sources such as silica,[18] these materials can be described as architectonic materials of nanoscale precision, so the general term "nanoarchitectonics" is used by researchers[19] to describe the mesoporous materials. The morphology of the mesoporous silica materials can be finely tuned by controlling the synthesis conditions, namely, the temperature, solution pH, surfactant-to-silica ratio, nature of the surfactants, and nature of the silica sources.[18] Methodology to prepare mesoporous silica via the template synthesis can be extended to preparation of various mesoporous metal phosphates.[20] Conversion of materials from silica to other materials is also possible. Matsukata and co-workers have recently developed rapid crystallization of MCM-41 by using a new evaporation-to-dryness technique using aqueous ammonia solution in a wide range of molar ratios of tetraethyl orthosilicate (TEOS), water, and surfactants.[21] There was no difference in the d_{100} values between as-prepared and calcined MCM-41, implying the formation of a highly dense silicate framework. The MCM-41 obtained after calcination

*Author to whom correspondence should be addressed.

shows a high degree of thermal stability and water resistance. Various compositional controls of organosilica frameworks have also been achieved by many other researchers.[22]

The scope of this work is to synthesis mesoporous material using TEOS as silicon source and heteroatom Zr is incorporated in Si frame work using organic source for metal Zr. After the introduction of Zr in Si-MCM-41 hydrothermally, surface acidity of the obtained Zr-MCM-41 is enhanced by sulfation and its catalytic efficiency is investigated. It is well known that zirconia, when modified with anions such as sulfate, forms a highly acidic or super acidic catalyst. In recent years, sulfated zirconia super acids have attracted increasing attention because these catalysts are found to be well suited for catalyzing reactions of industrially important organic transformations such as dehydration of alcohols, hydrocarbon isomerization, etherification and alkylation reactions.[23–30] However the non-uniform pore size and relatively small surface area of SO_4^{2-}/ZrO_2 may limit its potential application for catalyzing bulky molecules.[31] The application of MCM-41 and other mesoporous materials[32–35] which have uniform mesoporous and high surface area, as catalyst supports for SO_4^{2-}. It is greatly enhanced the catalytic properties and capabilities of SO_4^{2-}/ZrO_2-MCM-41 as strong acid catalysts for reactions containing bulky molecules. This is because such mesoporous materials, which have relatively small diffusion hindrance, can aid the diffusion of bulky organic molecules in and out of their mesoporous quite easily and enhanced acid sites.[32] Many superacid catalysts have been developed using silica, alumina and microporous zeolites as supporting materials.[24–30] Great effort has been focused on improving its surface acidity through surface and framework modifications. For instance, by introducing some strong acid sites like sulfuric ions,[36] sulfated zirconia[37] or heteropoly acids with Keggin structures[38, 39] onto the surface or inner channels of Si-MCM-41, the acidity of the material can be improved. Incorporation of heteroatom such as Cu, Zn, Al, B, Ga, Fe, Cr, Ti, V, Sn, and U into mesoporous silica framework has been widely investigated.[40–43]

The incorporation of foreign ions into the Si-MCM-41 framework for promoting surface acidity is interesting route. When Si ions in the Si-MCM-41 framework are partially substituted by other ions, such as Al^{3+}, Fe^{3+}, Ti^{4+}, Ga^{3+} and V^{5+}, a variety of framework modified mesoporous materials with larger surface, modified thermal stability and enhanced surface acidity may be obtained.[44–51] The Zr-based nanomaterials were used as a catalyst for acid catalyzed reactions,[52–55] and Zr is partially replacing Si ions in the Si-MCM-41 framework, in order to obtain Zr-containing mesostructured solids. Usually, the zirconium ions in mesostructured materials can be accessible to reactants because the majority of them are located on the surface of the pore walls, due to their trend to adopt high coordination numbers.[56, 57] There is a method[58] employed by surface grafting tetraneopentyl zirconium on the Si-MCM-41, indeed, the surface acidity of the resultant solids was enhanced; however, the grafting operation was carried out in a vacuum condition and is thus rather complex. In a sol–gel method zirconia and silica sources to obtain a mesocomposite with high zirconia content showing both Lewis and Bronsted acidity,[59] but it has very low porosity. In a work,[60] by doubly doping Si-MCM-41 by introducing Zr^{4+} into the framework and *in situ* sulfation of the surface, a long-range ordered Zr containing MCM-41 mesostructure with enhanced thermal stability was obtained. But, the Bronsted acidity of the resultant solids was not noticeably promoted. Therefore, the combination of a regular mesoporous structure and an enhanced surface acidity induced by the presence of zirconium is of particular interest and challenging. Many research groups have studied these systems and explored them in petroleum industry, particularly for isomerization of light alkanes.[61, 62] However; these catalysts are not exploited in the areas of fine chemicals synthesis. Therefore, a comprehensive investigation was undertaken on zirconia catalysts for organic synthesis and transformation reactions in the liquid phase. In the present work, foreign Zr^{4+} was introduced into the framework of Si-MCM-41 using a cationic surfactant-templated preparation method. The active super acid SO_4^{2-} component has been successfully supported on the surface of ZrO_2-MCM-41 to form a new SO_4^{2-}/ZrO_2-MCM-41 superacid catalyst. The sulfated materials were characterized and catalytic activity was investigated on dehydration of oximes and the results are reported.

2. EXPERIMENTAL DETAILS

2.1. Catalyst Preparation

2.1.1. Si-MCM-41

Si-MCM-41 sample was prepared using tetraethyl orthosilicate (TEOS) as a precursor. The preparation method was described by Salas et al.[60] About 7.2 g of the surfactant, cetyltrimethylammonium bromide (CTAB) was dissolved in doubly distilled warm water. 59.2 ml of NH_3 (28%) was added to this solution under stirring. 14.4 ml of TEOS was added drop wise, to the surfactant solution with vigorous stirring for 3 hr to form a gel. The resultant gel was transferred to a Teflon lined autoclave (150 ml) and heated at 80 °C for 48 hr. The white solid material was filtered and washed with ethanol twice followed by doubly distilled water, and then dried at 100 °C for 24 hr. Finally, the resultant solid was calcined in air at 650 °C (heating rate 1 °C min^{-1}) for 6 hr.

2.1.2. Si-Zr-MCM-41

Zr-MCM-41 samples were prepared using organic sources like tetraethyl orthosilicate (TEOS) and zirconium *n*-propoxide (ZP) (70%) as the precursors with a molar ratio $SiO_2/ZrO_2 = 20$. The preparation of solution I was

as follows: 1.44 ml of zirconium *n*-propoxide (ZP) was dissolved in 14.4 ml of tetraethyl orthosilicate (TEOS) by stirring for 3 hr. The solution II was prepared by dissolving 7.2 g of the surfactant, template cetyltrimethylammonium bromide (CTAB) in doubly distilled warm water. 59.2 ml of NH_3 (28%) was added to this solution under stirring. The solution I was added drop by drop, to the solution II with vigorous stirring to form a gel, and the stirring continued for 2 hr. The resultant gel was transferred to a Teflon lined autoclave (150 ml) and heated at 80 °C for 48 hr. The crystallized product was filtered and washed with ethanol followed by deionized water, and then dried at 100 °C for 24 hr. Finally, the solid was calcined in air at 650 °C (1 °C min^{-1} heating rate) for 6 hr. This material was denoted as SiZr20. Similarly SiZrx was prepared (where $x =$ Si/Zr = 10, 30). The surface acidity of SiZr20 solid was enhanced by treating with sulfating agents H_2SO_4 and ammonium sulfate. It was immersed into 0.5 M H_2SO_4 solution and stirred at room temperature for 30 min. The resultant material was then filtered off, dried in water bath. The obtained solid was then oven dried at 100 °C over night and calcined at 550 °C in air for 3 hr to form SO_4^{2-}/ZrO_2-MCM-41. It was denoted as SAZrM. The SiZr20 solid was immersed in an aqueous solution of ammonium sulfate (AS) with different concentrations, i.e., 4%, 8% and 12% wt.% of ammonium sulfate and stirred at room temperature for 30 min. The resultant material was then filtered off, dried in water bath. The obtained solid was then dried in oven at 100 °C over night. Finally, all the samples were calcined in air flow (20 cm^3/min) at 550 °C for 3 hr to obtain ASZrM and samples were denoted as 4ASZrM, 8ASZrM and 12ASZrM.

2.2. Characterization

The XRD powder diffraction patterns of the calcined mesoporous sulfated Zr-MCM-41 molecular sieves were obtained with a Stereoscan diffractometer using nickel-filtered CuKα radiation and a liquid nitrogen cooled germanium solid-state detector. The diffractograms were recorded in the 2θ range of 1.03–9.99° in the steps of 0.02° with a count time of 15 s at each point for molecular sieves. The specific surface area, pore volume and pore size distribution were measured by nitrogen adsorption at 77 K using an ASAP-2010 porosimeter from Micromeritics Corporation, GA. The samples were degassed at 623 K and 10^{-5} torr overnight prior to the adsorption experiments. The mesoporous volume was estimated from the amount of nitrogen adsorbed at a relative pressure of 0.5 (p/p_o) by assuming that all the mesopores were filled with condensed nitrogen in the normal liquid state. Pore size distribution was estimated using the Barrett, Joyner and Halenda (BJH) algorithm (ASAP-2010) available as built-in software from Micromeritics. The temperature programmed desorption of ammonia (TPD-NH_3) was carried out to determine the acidity of the material. 0.2. g of sample was firstly loaded in the microreactor (Micromeritics Instrument Corporation) and heated in flowing He (20 cc per min) at 550 °C for 2 hr. The sample was cooled to 100 °C. Now the He gas flow was stopped and NH_3 gas was allowed to flow with the flow rate of 20 cc per min for 30 min at 100 °C. To remove the free NH_3, the sample was flushed out for 2 hr with He gas (20 cc per min) at 100 °C. TPD is started by allowing carrier gas He with the flow rate of 40 cc per min from room temperature to 900 °C at a linear heating rate of 10 °C per min. The desorption of NH_3 was detected by a Thermal Conducting Detector (TCD). The graph is drawn between TCD Signal (a.u.) versus Temperature. The amount of NH_3 desorbed (in mmol/g) is correlated with the strength of acid present in the material. The element sulfur in impregnated sulfate on mesoporous material and the reusability of the catalyst were determined by XRF using a Philips (PW 1480) wavelength dispersive spectrometer; with a rhodium tube operated at 50 kV a PE crystal and a scintillation counter. Samples were pressed as homogeneous tablets of the compressed (12 MPa) powder of the catalyst system. The mesoporous molecular sieves were analyzed to find out the elements present in it by using Elementar Vario EL III-Germany.

2.3. Catalytic Study

To investigate the catalytic activity of the SAZrM the dehydration of cyclohexanone oxime was carried out in liquid-phase at 150 °C in a 50 ml three necked round bottom flask equipped with a reflux condenser and a magnetic stirrer. The reactor was immersed in an oil bath. A typical reaction run was as follows: under moisture free N_2 atmosphere 0.2 g catalyst was added in a solution of 15 mmol of cyclohexanone oxime in 10 ml of acetonitrile. This reaction mixture was heated to 150 °C and stirred for required time. The identification of product was performed on a Shimadzu GC-MS-QP 5000 with a PE-5 capillary column: scan mode 40–400 amu and also by comparing with the authentic standard. The product was also analyzed by HPLC Shimadzu CLASS-VP V6.4 SP1 with UV detector and FTIR. Conversion of oxime was determined on its disappearance in the reaction mixture.

In another reaction the dehydration of salicylaldoxime was carried out in the liquid phase in a sealed reactor immersed in a thermo-state oil bath and a magnetic stirrer. A typical reaction run was as follows: Under moisture free N_2 atmosphere 0.2 g catalyst, pre-activated in air at 400 °C (to remove the adsorbed water molecule), was suspended in a solution of 5 mmol of salicylaldoxime in 5 ml of solvent. The reaction mixture was heated to the desired temperature and stirred. Samples withdrawn periodically were analyzed by Shimadzu GC-17A, gas chromatograph fitted DB-55 capillary column with FID detector using nitrogen as the carrier gas. The identification of products was performed on a Shimadzu (Gas chromatography-Mass Spectroscopy) GC-MS-QP 5000 with a PE-5 capillary column: scan mode 30–400 amu and also by comparing

with the authentic standard. The product was also analyzed by HPLC Shimadzu CLASS-VP V6.4 SP1 with UV detector and FTIR. Conversion of oxime was determined on its disappearance in the reaction mixture. The regeneration of the spent catalyst from the first run was filtered and washed with acetonitrile three times and calcined at 450 °C for 4 hr in an air to reactivate the catalyst. It was used for consecutive runs and examined by XRF to find out the amount of sulfur on the surface of the material. The spent catalysts were also analyzed by CHNS elemental analysis method.

3. RESULTS AND DISCUSSION

3.1. Characterization of the Catalysts

3.1.1. Structure and Textural Properties of the Sulfated Zr-MCM-41

Figures 1(a)–(c) and (h) showed the XRD pattern of the calcined SiZrX (calcination temperature 650 °C for 6 h) with different Si/Zr molar ratios (Si/Zr = 10, 20 and 30) and sulfated Zr mesoporous materials. Peaks corresponding to the (1 0 0), (1 1 0) were observed and they were indexed to the hexagonal structure of typical mesoporous MCM-41 materials. The intensities of the diffraction peaks decreased with the increase in zirconium content beyond the optimum Si/Zr ratio. Among the calcined samples (Si/Zr = 10, 20 and 30) Si/Zr = 20 showed the highest intensity for (1 0 0) while, the sample with Si/Zr = 10 showed the lowest intensity, indicating that the zirconium content in the solid has an important effect on the structural ordering of the resultant materials. Therefore, by incorporation of an optimized amount of zirconium ions into the framework, the well ordered structure can be obtained than the high Zr content material. With low zirconium content, (Si/Zr = 30) this improvement was not significant; however, a high zirconium content resulted in a poor structural regularity, as in the case of Si/Zr = 10, due to large structural strain. Among the Si/Zr ratio 10, 20 and 30 the molar ratio Si/Zr = 20 was optimal, corresponding to the best structural ordering.[63] In Table I the related structural data derived from the XRD analysis and textural property measurements showed. As the Si/Zr molar ratio decreased from 30 to 10, the (1 0 0) peak position slightly shifted towards smaller values when compared with as-synthesized Zr-MCM-41,[60] thus the distance of the (1 0 0) interplanar spacing and the lattice cell parameter (a_0) increased. The wall thickness (t) slightly increased with the increase in the zirconium content, indicating the incorporation of zirconium into the framework. The X-ray diffractograms of sulfated Zr-MCM-41 showed in Figures 1(d)–(g) that the (100) peak lost its sharpness and broadened when the sulfate loading increased. The intensity of (110) plane was very low or even disappeared evidenced that the clogging of ordered hexagonal structure occurred due to high sulfate loading.

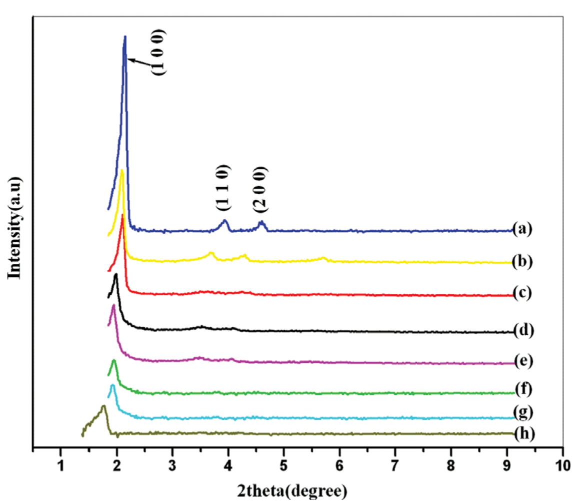

Figure 1. XRD: (a) Si-MCM-41, (b) SiZrM20, (c) SiZrM30, (d) SAZrM, (e) 4ASZrM, (f) 8ASZrM, (g) 12ASZrM, (h) SiZrM10.

The N_2 adsorption–desorption properties (BET) of the samples of Zr-MCM-41 materials calcined at 550 °C were determined; the results were illustrated in Figure 2. Based on the IUPAC classification, they were assigned to Type IV isotherm. A sharp step at a relative pressure p/p_0 0.22–0.30 was observed in all the samples (SiZr10, SiZr20 and SiZr30) which revealed highly ordered mesoporous nature and uniform pore channels. The region $p/p_0 < 0.2$ was due to a monolayer adsorption of nitrogen on the walls of the mesopores. The region $p/p_0 = 0.20$ to 0.30 characterized by the capillary condensation inside the mesopores. The inflection started at 0.2 related to the diameter of the mesopores and the sharp increase indicates the pore width of the mesopores. However the region $p/p_0 > 0.3$ was due to a multilayer adsorption on the outer surface of the material. SiZrMx showed two sharp capillary condensation regions due to the presence of mesopores and cross-linked inter particle pores in the region p/p_0 between 0.2 and 0.3 and 0.9–1.0 respectively. It is evidenced that the mesoporous material was in nanoscale with ordered frame work. These characteristic two peaks indicated the presence of uniform, inter and intra particle pores in the Zr mesoporous material.[64,65] The shape and the sharpness of the isotherms vary with the zirconium content. The N_2 adsorption and desorption isotherms are almost overlapped but they are gradually separated as the zirconium content increases.[65] The organic sources TEOS and ZP facilitated the formation of nanometer sized particle in Zr-MCM-41. But Si-MCM-41 synthesized without ZP exhibited only one sharp condensation peak revealed that there was no detectable inter particle porosity rather micrometer sized particle.

The pore diameter (dp) (Fig. 3) corresponding to the main peak in the pore size distribution profile slightly increased with the zirconium content until the Si/Zr molar

Table I. Structural and Textural characteristics: Si-MCM-41, SiZrM10, SiZrM20, SiZrM30, SAZrM, 4ASZrM, 8ASZrM, 12ASZrM.

Sample (ICP)	Surface Area[1] (m^2/g)	Pore volume[1] (cm^3/g)	dp (nm)[1]	$d_{(100)2}$ (nm)	a_o^2 (nm)	t (nm)
Si-MCM-41	921	1.03	2.36	**3.66**	4.23	1.87
SiZrM30 (25.493)	882	1.07	2.36	**3.67**	4.24	1.88
SiZrM20 (18.750)	867	1.12	2.38	**3.73**	4.31	1.93
SiZrM10 (11.423)	584	1.14	2.39	**3.75**	4.55	2.01
SAZrM	710	1.04	2.36	**3.74**	4.32	1.96
4ASZrM	642	1.10	2.37	**3.75**	4.33	1.96
8ASZrM	628	0.97	2.37	**3.74**	4.31	1.95
12ASZrM	386	0.94	2.34	**3.75**	4.33	1.99

Notes: [1]The values obtained from N_2 adsorption–desorption studies; [2]The results obtained from XRD analysis.

ratio reached 10. However, the average pore diameter (dpa) linearly increases as the Si/Zr molar ratio decreased from 30 to 10, indicating collapse some mesopores in the solids with high zirconium content. At low zirconium contents, a narrow pore size distribution was obtained while at high zirconium contents the pore size distribution became broad. The high zirconium content also led to the reduction in surface area. These observations revealed that the incorporation of Zr into Si frame work strongly affected the textural properties of the materials. It ascertained the presence of bimodal pore system in the SiZrMx. The sharp peak at 23.8 Å was the primary and at 39.7 Å was the secondary and the later was less dominating pores system in the material. The N_2 adsorption–desorption study of sulfated materials indicated that the intensity of primary pore system decreased and secondary pore system eliminated and surface area decreased due to sulfation.[60] It was evidenced the impregnated sulfate occupied the secondary pores and contributed to generate more acidity. The textural data of the materials was reported in Table I.

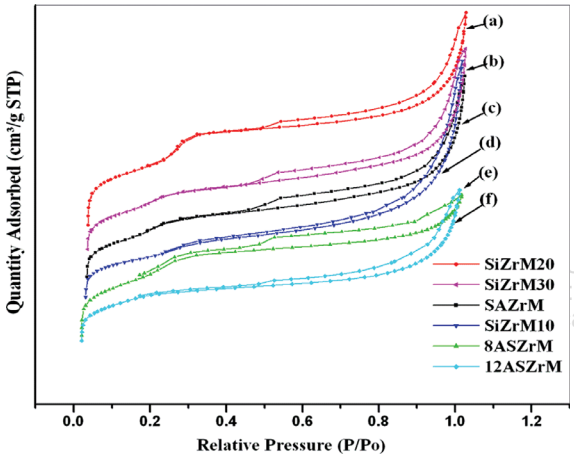

Figure 2. BET isotherm: (a) SiZrM20, (b) SiZrM30, (c) SAZrM, (d) SiZrM10 (e) 8ASZrM, (f) 12ASZrM.

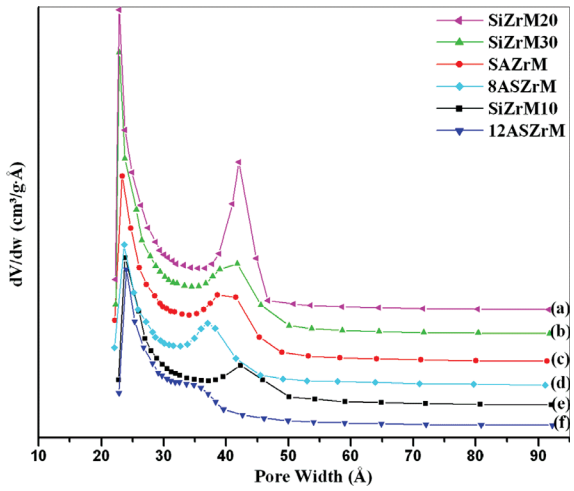

Figure 3. Pore size distributions: (a) SiZrM20, (b) SiZrM30, (c) SAZrM, (d) 8ASZrM, (e) SiZrM10, (f) 12ASZrM.

3.1.2. *Total Surface Acidity by Temperature-Programmed Desorption of Ammonia (NH_3-TPD)*

Ammonia TPD was widely used to determine the total acidity of solids. The amount of ammonia desorbed at some characteristic temperatures is taken as a measure of the number of acid centers while the temperature range in which the ammonia is desorbed is an indicator of the strength of the acid sites. It can distinguish sites by sorption strength only but not Lewis from Bronsted type sites.[66,67] For mesoporous silica zirconia, the NH_3-TPD curves were broad and complete desorption was reached (Fig. 4).

There were two temperature maxima on all the samples indicating the presence of two different types of acid sites. The total amount of ammonia desorbed in the case of sulfated samples was much higher than that of SiZrM20. This clearly indicated the impregnated sulfate ions strongly influenced the total surface acidity of the materials. The acid strength distribution at various temperature regions are summarized in Table II. In general the region below 400 °C in the NH_3-TPD spectrum was called as Low Temperature (LT) region and above 400 °C was called as High Temperature (HT) region. In the sulfated materials the major acidity was observed in strong (HT)

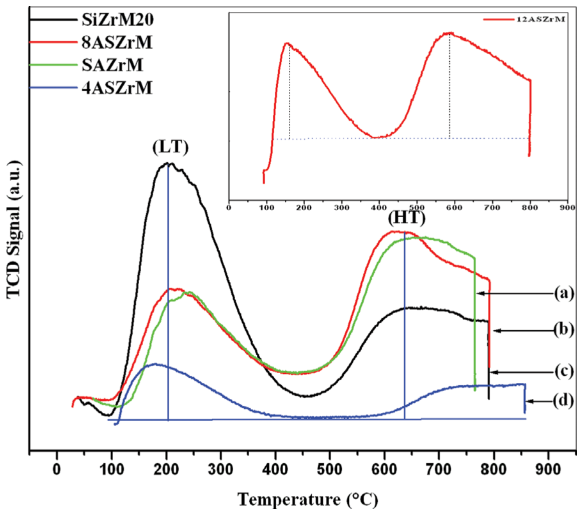

Figure 4. NH_3-TPD Profile: (a) SAZrM, (b) 8ASZrM, (c) SiZrM20, (d) 4ASZrM, In-set: 12ASZrM.

region (> 400 °C). The NH_3-TPD analysis showed the peaks at high temperature region occur due to desorption of ammonia from strong acid sites[68] which are catalytically important.[69]

Generally the HT indicated the material possess strong acidity in it. The SiZrM20 showed LT (weak acidity) region peak. On comparing the catalytic activity of SiZrM20 (yield = 63%) and SAZrM (yield = 96%) in dehydration of salicylaldoxime, which is shown that the yield depends on the amount of acidity present in the material. The SiZrM20 lacks in HT acidity and hence it produced less yield. After the sulfation the strong acidity generated on SiZrM20 which created more number of active site and hence the selectivity and yield increased remarkably. The total acidity of SiZrM20 and sulfated Zr-MCM-41 materials were shown in Table II can be correlated with the Tables III and IV. The HT acid strength of SAZrM is 1.5 times greater than SiZrM20 after sulfation. Hence SAZrM shows 100% conversion of oxime and 96% selectivity of nitrile. The less conversion and selectivity shown by 12ASZrM material may be due to the blocking of excess sulfates in pore channels, which makes the hindrance for diffusion of oxime.

Table II. NH_3-TPD Profile: SiZrM20, SAZrM, 4ASZrM, 8ASZrM, 12ASZrM.

	Acid strength NH_3-desorption (mmol/g)		
Catalysts	Medium Strong acid (LT) 200–400 °C	Strong acid (HT) > 400 °C	Total acidity (mmol/g)
SiZrM20	0.1836	0.1289	0.3125
SAZrM	0.1482	0.295	0.4432
4ASZrM	0.1315	0.2012	0.3327
8ASZrM	0.1422	0.289	0.4312
12ASZrM	0.1415	0.2664	0.4079

Table III. Effect of catalysts on dehydration of cyclohexanone oxime.

Catalyst	Conversion of oxime percentage	Selectivity of caprolactam percentage
Si-MCM-41	NIL	NIL
SiZrM30	27	41
SiZrM20	44	52
SiZrM10	33	38
4ASZrM	47	54
8ASZrM	73	76
12ASZrM	62	72
SAZrM	100	83

Note: Reaction conditions: 15 mmol cyclohexanone oxime, 0.20 g of catalyst, 10 ml Acetonitrile: 150 °C: 3 h.

Table IV. Effect of catalysts on dehydration of salicylaldoxime.

Catalyst	Conversion of oxime (%)	Selectivity of nitrile (%)
Si-MCM-41	22	42
SiZrM30	34	56
SiZrM20	41	63
SiZrM10	46	57
4ASZrM	67	76
8ASZrM	95	84
12ASZrM	64	82
SAZrM	100	96

Note: Reaction Conditions: 5 mmol salicylaldoxime, 0.20 g of catalyst, 20 ml Acetonitrile: 150 °C: 6 h.

3.1.3. FT-IR Spectroscopy

The IR spectra of sulfated zirconia mesoporous materials are recorded in the spectral region of 400 to 4000 cm^{-1} and present in Figure 5. It showed absorption band with a maximum at around 3460 cm^{-1} in the OH stretching region which is attributed to Si—OH or the band of water molecule and at 1655 cm^{-1} is assigned to –OH bending vibration.[70] Peak at 1097 cm^{-1} is for Si—O—Si asymmetric stretching vibration and at 971 cm^{-1} indicated the

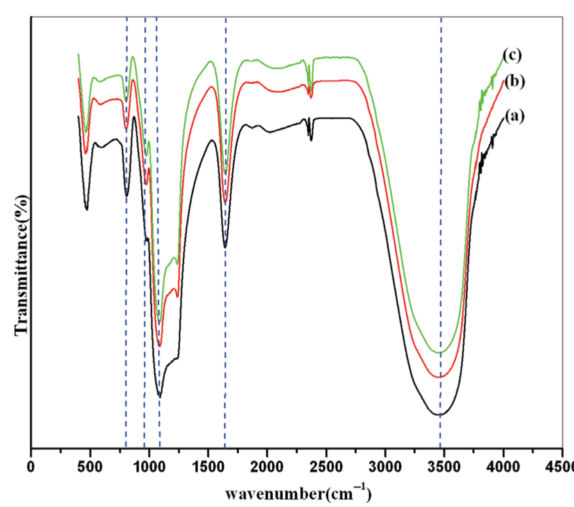

Figure 5. FT-IR: (a) SiZrM10, (b) SiZrM20, (c) SiZrM30.

presence of Si—O—Zr.[71] The band at 1017 cm^{-1} is characterized for Si—O—Si asymmetric stretching vibration. But in this study there was a shift from 1017 to 1097 cm^{-1}. It might be due to introduction of Zr in Si frame work. The band at 797 cm^{-1} corresponds to Si—O—Si symmetric stretching vibration mode and at 587 cm^{-1} ascribed for O—Zr—O vibration mode.[71] The FTIR result revealed the Zr ion inserted in to the Si frame work.

3.1.4. Scanning Electron Microscopy (SEM)

The morphological features of zirconium incorporated mesoporous materials and sulfate loaded mesoporous material were investigated by scanning electron microscope (SEM). Figure 6 presents the SEM image of SiZrM20. It is observed that the aggregation of particles in the material which indicates that the material is mesoporous material. The material is having sponge like structures and there is no definite morphology is observed in the image. The EDAX of the material SiZrM20 shows the presence of Si and Zr for their respective Kα signals confirming their presence in the catalyst. The SEM image of sulfated Zr-MCM-41 (Fig. 7) shows the presence of aggregated particles distributed unevenly. The impregnated sulfate over the silica host material is evidenced by EDAX, XRF and CHNS elemental analysis.

3.1.5. Dehydration of Cyclohexanone Oxime

The dehydration of cyclohexanone oxime was carried out and the product was analyzed by GC-MS, HPLC and FTIR. It was known that the selectivity of industrially important caprolactam depends strongly on the acidity of the catalyst. It has been reported that the intermediate strength of acid sites were responsible for the selectivity of lactam.[72, 73] The strong acid sites present in the catalyst were the reason for the formation of polymeric products and coke formation on the surface of the catalyst. It led to rapid deactivation of the strong acid sites and thereby decreased in lactam selectivity.[72, 73] The oxime conversion and lactam selectivity depended on the medium strength acid sites indicated in ammonia desorption study between the temperature range 200 and 350 °C.[74] Chaudhari et al.[75] proposed that the cyclohexanone oxime undergoes Beckmann rearrangement and forms lactam under moderate acidic condition. It can be shown that the strong acidity in the material was the reason for the rapid formation of caprolactam and polymeric products.

The product collected at 3rd hour showed major peak at RT = 6.49 at m/z = 112.55, 83.01, 66.95 and 54. It was compared with authentic and the product caprolactam was confirmed. The product collected after 3rd hour

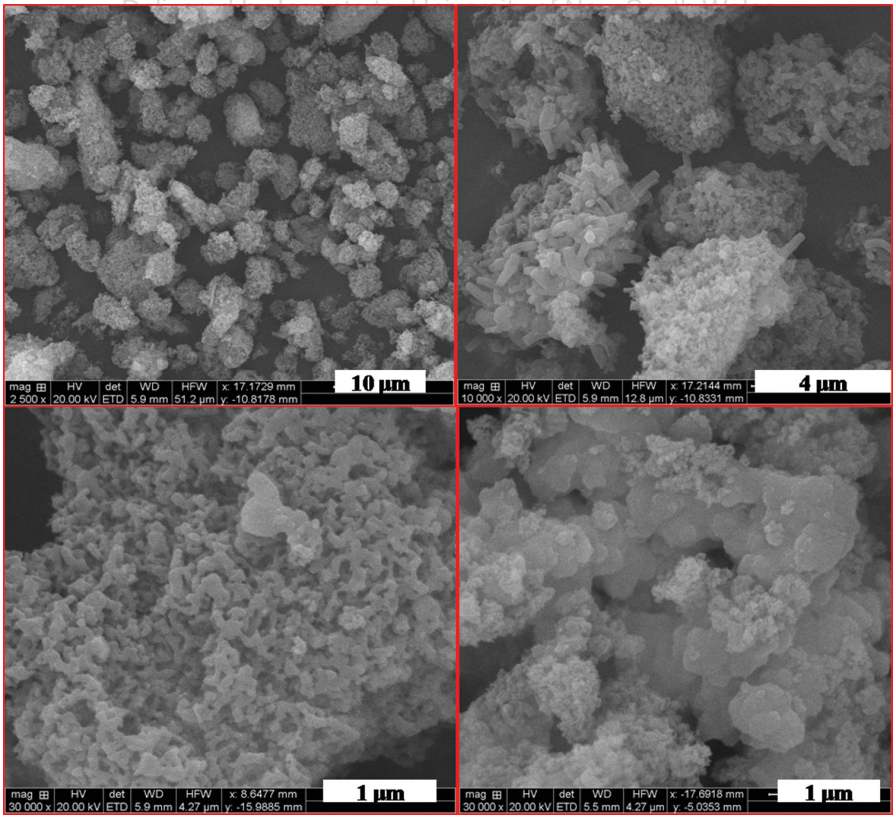

Figure 6. SEM Image: SiZrM20.

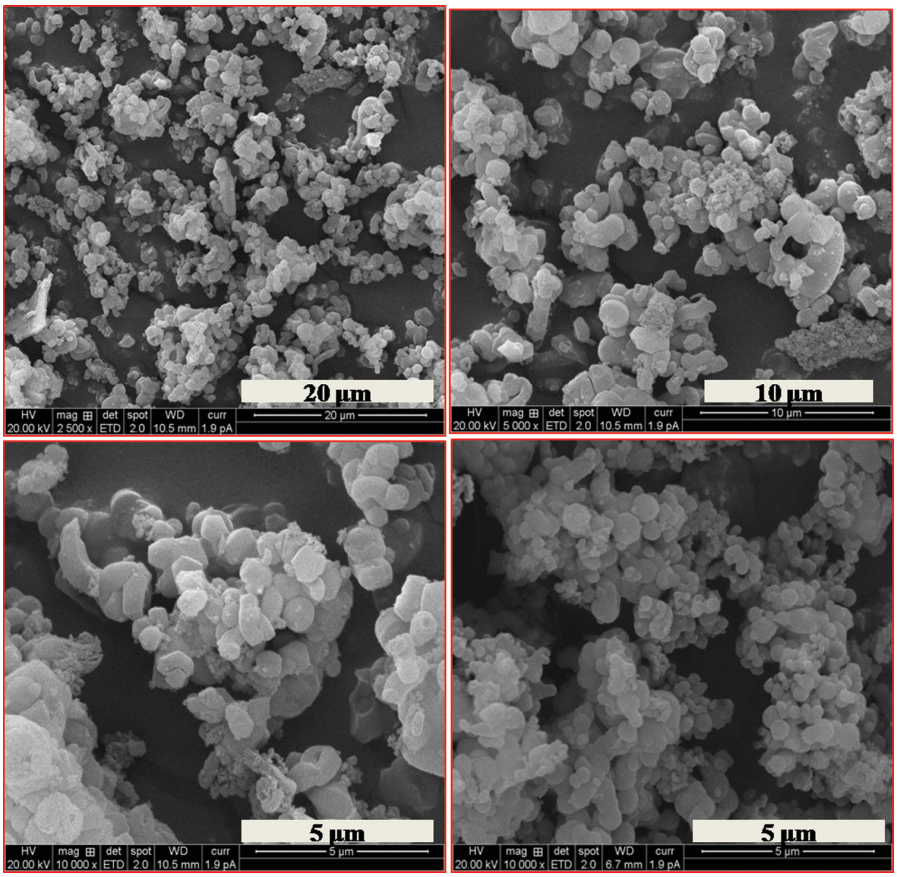

Figure 7. SEM Image: SAZrM.

was analyzed by GC-MS. Higher $m/z = 454$, 595, 623 and 649 peaks observed whichillustrated the formation of polymerized product of caprolactam. FT-IR of caprolactam (KBr, v/cm^{-1}) band at 1567 for N—H bending, 1154 for aliphatic C—N stretching and band at 1706 for C=O stretching, 3400–3250 cm^{-1} for 1° or 2° N—H stretching which is overlapped with OH– stretching mode. These data showed the formation of caprolactam. The HPLC result showed 83% of caprolactam and 13% byproducts evidenced that the material possess strong acid sites along with medium acid sites. The catalytic activity of all the catalysts in dehydration of cyclohexanone oxime showed in Table III.

3.1.6. Dehydration of Salicylaldoxime

The acidity nature of the sulfate impregnated Zr-MCM-41 can be investigated with the dehydration of Salicylaldoxime into nitrile as a probe molecule. This discussion can be supported by the surface studies and NH_3-TPD profile. The activity and selectivity of the reaction were not only depending on the strength of acid sites, but long range order pore structure and large surface area also the deciding factures. If the catalyst does not possess strong acid sites or HT acidity, salicylaldoxime (containing sensitive –OH at C-2) will not undergo dehydration and produces nitrile (Fig. 8 Route. 1), because weak medium acid sites will produce only Beckmann rearrangement

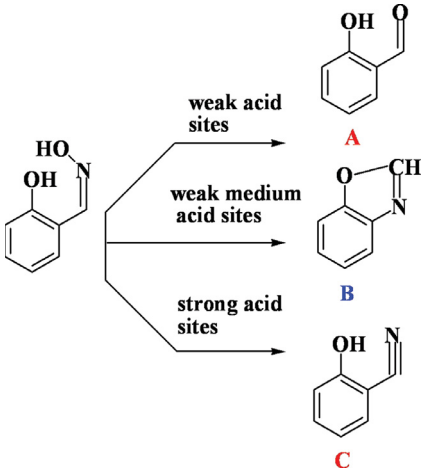

Figure 8. Dehydration of salicylaldoxime.

product (Fig. 8 Route. 2) and weak acid catalyst produces Salicylaldehyde (Fig. 8 Route. 3).

The effect of catalysts on dehydration of salicylaldoxime is presented in Table IV. The SAZrM showed 100% conversion of oxime while the unloaded SiZr20 showed only 41% conversion, 73% selectivity of nitrile. After sulfation the strength of acid sites on the material increased drastically. The conversion and selectivity increased with the increase in acid strength, however the 12ASZM with high acid strength showed only 64% conversion. The excess sulfate loading on mesoporous sieve might led to pore blocking, disorder in morphology and hence poor catalytic activity showed by the material. At the same time SAZrM gave 100% conversion of oxime and 96% selectivity of nitrile which revealed the reactant diffused well without any hindrance and underwent dehydration smoothly. The catalyst 8ASZrM showed 91% selectivity and its activity was almost same as SAZrM. The more the amount of strong acid centers the higher the nitrile formation. It is noted that the dehydration of oxime took place over strong acid sites present in SAZrM. From these results it can be interpreted that the large surface area provided more number of acid sites and the mesopores facilitated the substrate to undergo diffusion and thereby the high % of product selectivity is achieved. The mesoporous materials with high surface area are good catalysts and large potential application in the fine chemical industry, adsorption processes and in petroleum refinery industry.[76]

The plausible mechanism (Fig. 9) was proposed that the protonation of oxime-hydroxide took place. The removal of water molecule and deprotonation took place simultaneously followed by formation of nitrile. The dehydration products were analyzed cautiously to confirm the nature of the acid sites generated on sulfated materials.

The elaborate kinetic study of dehydration of oxime was carried out to find the optimal reaction conditions. The effect of solvent in liquid phase system is reported in Table V. The dehydration of salicylaldoxime took place well in polar aprotic solvent acetonitrile than in non polar aprotic solvent. This is because the oxime was brought to the active centers of the catalyst surface effectively by the polar aprotic acetonitrile than toluene and acetone.

The influence of reaction temperature on conversion and selectivity was investigated at 90, 120 and 150 °C. Salicylaldoxime conversion and selectivity of salicylonitrile at various temperatures were presented in Table VI. When the temperature increased to 150 °C the conversion 100% and selectivity of nitrile 96% reached. Hence for this liquid

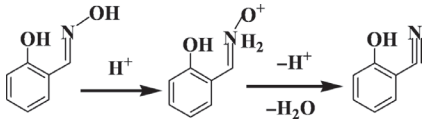

Figure 9. Plausible mechanism: Dehydration of Salicylaldoxime by SAZrM.

Table V. Effect of solvent in dehydration of salicylaldoxime.

Solvent	Dielectric constant	Conversion of oxime (%)	Selectivity of nitrile (%)
Acetone	21.01	66	72
Acetonitrile	36.64	100	96
Toluene	3.9	72	89.7

Notes: Reaction Conditions: 5 mmol salicylaldoxime, 0.20 g of catalyst SAZrM, 20 ml solvent: 150 °C: 6 h.

Table VI. Effect of reaction temperature in dehydration of salicylaldoxime.

Temp °C	Conversion of oxime (%)	Selectivity of nitrile (%)
90	43	62
120	67	76
150	100	96

Notes: Reaction Conditions: 5mmol salicylaldoxime, 0.20 g of catalyst SAZrM, 20 ml Acetonitrile: 6 h.

phase system the optimum temperature was found to be 150 °C.

The reaction time was optimized and presented in Table VII. The sample was withdrawn from the reaction mixture after 2 h and examined. The conversion was only 31%. The conversion increased gradually with increase in time. Oximes might require much time to diffuse and undergo the reaction. The selectivity was reached 96% at 6 h, after 8 h the selectivity of nitrile decreased due to formation of higher molecular weight substances.

The GC-MS results showed the peak at RT = 6.26 were as follows: $m/z = 119$, 89.5, 76, 63 and 50. The FT-IR spectra of nitrile was as follows: (KBr, v/cm^{-1}) 3554-phenolic –OH stretching, 3167-Aromatic C—H stretching, 2252-aromatic nitrile C═N, 2066-combination band for aromatics, 1630-Aromatic ring stretching, 1424 C═C—C stretching, 1375-phenolic –OH bending, 1267-phenolic–O—H stretching, 920-aromatic C—H (out of plane) bending, 759 −1,2 substitution in aromatic ring stretching. These results ascertained the formation of 2-hydroxy benzonitrile (salicylonitrile).

3.1.7. Leaching Study

The elements present in the sulfated materials quantified by XRF. This technique is quiet convenient to determine the elements such as silicon (Si), Zirconium (Zr) and sulfur (S) present in the material. The reusability of the catalyst SAZrM (S-1.899%) was investigated by XRF (Table VIII).

Table VII. Effect of reaction time in dehydration of salicylaldoxime.

Time (h)	Conversion of oxime	Selectivity of nitrile
2	31	45
4	74	67
6	100	96

Notes: Reaction Conditions: 5 mmol salicylaldoxime, 0.20 g of catalyst SAZrM, 20 ml Acetonitrile: 150 °C.

Table VIII. Leaching study.

Runs	Fresh	1	2	3	4
Sulfur content CHNS (XRF) wt%	1.817(1.899)	1.781(1.887)	1.779(1.884)	1.776(1.88)	1.77(1.877)
% Selectivity of Nitrile	96	91	89	90	88

Notes: Reaction Conditions: 5 mmol salicylaldoxime, 0.20 g of catalyst SAZrM, 20 ml Acetonitrile: 150 °C: 6 h/run.

The sulfur content reduced (from 1.899% to 1.879%) by 1.05% for the catalyst in the first run. The reactivated catalyst after four runs showed only 1.15% sulfur leaching. Therefore, the leaching study revealed the sulfur loaded on the surface which was not interacting with Zr expelled after the first run. But in consecutive runs sulfur interacting with Zr ion of the mesoporous sieve did not show any leaching. This leaching study results also agree with CHNS elemental analysis results

4. CONCLUSION

In summary we have established super acidity in Si-MCM-41 by frame work incorporation of Zr and subsequent sulfation. Catalysts and its catalytic activity were studied in dehydration of oximes. From the pore analysis results it is attributed that the SiZrMx possesses inter mesopores and intra pores which make the material as bimodal. SAZrM super acid catalyst could catalyze the dehydration of salicylaldoxime and cyclohexanone oxime. Even for other acid catalyzed reactions the catalyst could be a convenient substitute for mineral acids. The presences of bimodal pore system in SAZrM, it could be the effective catalyst for acid catalyzed reactions of sterically crowded substrates compared to microporous materials.

Acknowledgment: The authors are thankful to the Department of chemistry, (DST) Anna University Chennai and Indian Institute of Technology-Madras (SAIF) for providing the instrumentation facilities.

References and Notes

1. L. Souzana, K. Georgia, P. Chrysa, and K. G. Athanasios, *J. Nanosci. Nanotechnol.* 3, 697 (**2011**).
2. S. Shylesh, K. P. Mahendra, J. R. Lekh, C. H. Srilakshmi, and A. P. G. Singh, *J. Nanosci. Nanotechnol* 3, 497 (**2011**).
3. B. Naik, S. Hazra, P. Muktesh, V. S. Prasad, and N. Ghosh, *N. Sci. Adv. Mater.* 3, 1025 (**2011**).
4. X.-B. Tang, L.-S. Qiang, J. Ma, Y. Li, D.-Y. Tang, and Y.-L. Yang, *Sci. Adv. Mater.* 3, 1019 (**2011**).
5. R. Jayshree, R. Shukla, S. Chandramouleeswaran, T. Mukherjee, and A. K. Tyagi, *Nanosci. Nanotech. Lett.* 4, 693 (**2012**).
6. M. Miyahara, A. Vinu, K. Z. Hossain, T. Nakanishi, and K. Ariga, *Thin Solid Films* 499, 13 (**2006**).
7. M. Miyahara, A. Vinu, and K. Ariga, *Mater. Sci. Eng.* 27, 232 (**C 2007**).
8. A. Vinu, M. Miyahara, and K. Ariga, *J. Nanosci. Nanotechnol.* 6, 1510 (**2006**).
9. M. Miyahara, A. Vinu, and K. Ariga, *J. Nanosci. Nanotechnol.* 6, 1765 (**2006**).
10. K. Ariga, A. Vinu, and M. Miyahara, *Curr. Nanosci.* 2, 197 (**2006**).
11. A. Vinu, M. Miyahara, K. Z. Hossain, M. Takahashi, V. V. Balasubramanian, T. Mori, and K. Ariga, *J. Nanosci. Nanotechnol.* 7, 828 (**2007**).
12. M. Shanthini, N. Narayanan, M. S. S. Chandra, S. Sethuraman, and K. Uma Maheswari, *J. Biomed. Nanotechnol.* 9, 907 (**2013**).
13. F. Tang, L. Li, and D. Chen, *Adv. Mater.* 24, 1504 (**2012**).
14. Z. Li, J. C. Barnes, A. Bosoy, J. F. Stoddart, and J. I. Zink, *Chem. Soc. Rev.* 41, 2590 (**2012**).
15. N. Qureshi, G. Umarji, M. Shinde, R. Vivek, B. Lalit, M. Uttam, and A. Dinesh, *Mater. Expr.* 3, 79 (**2013**).
16. L. Xiayi, L. Wei, Z. Xiaolu, L. Xiaohua, and W. Xuemei, *Nanosci. Nanotech. Lett.* 5, 297 (**2013**).
17. J. Chen, J. Wu, C. Li, Y. Zhou, K. Qasim, X. Zhang, and W. Lei, *Nanosci. Nanotechnol. Lett.* 5, 178 (**2013**).
18. K. Ariga, A. Vinu, Y. Yamauchi, Q. Ji, and J. P. Hill, *Bull. Chem. Soc. Jpn* 85, 1 (**2012**).
19. K. Ariga, M. Li, G. J. Richards, and J. P. Hill, *J. Nanosci. Nanotechnol.* 11, 1 (**2011**).
20. N. Ikawa, M. Iwata, Y. Oumi, T. Kimura, and T. Sano, *J. Nanosci. Nanotechnol.* 9, 627 (**2009**).
21. S. Inagaki, Y. Aratani, S. Nakata, Y. Yashiro, Y. Sekine, E. Kikuchi, and M. Matsukata, *Bull. Chem. Soc. Jpn.* 82, 606 (**2009**).
22. N. Mizoshita, T. Tani, and S. Inagaki, *Chem. Soc. Rev.* 40, 789 (**2011**).
23. K. Arata, *Adv. Catal.* 37, 165 (**1990**).
24. G. D. Yadav and J. Nair, *J. Microporous Mesoporous Mater.* 33, 1 (**1999**).
25. Y. D. Xia, W. M. Hua, Y. Tang, and Z. Gao, *Chem. Commun.* 1899 (**1999**).
26. T. Jin, T. Yamaguchi, and K. Tanabe, *J. Phys. Chem.* 90, 4794 (**1986**).
27. G. D. Yadav and Kirthivasan, *J. Chem. Soc. Chem. Commun.* 203 (**1995**).
28. M. Hino and K. Arata, *J. Chem. Soc. Chem. Commun.* 1148 (**1979**).
29. F. R. Chen, G. Coudurier, J. F. Joly, and J. C. Vederine, *J. Catal.* 143, 616 (**1993**).
30. T. Lei, J. S. Xu, Y. Tang, W. M. Hua, and Z. Gao, *Appl. Catal. A: General.* 192, 181 (**2000**).
31. Q.-H. Xia, K. Hidajat, and S. Kawi, *Chem. Commun.* 2229 (**2000**).
32. S. Biz and M. L. Occeli, *Catal. Rev.-Sci. Eng.* 40, 329 (**1998**).
33. S. Kawi and M. W. Lai, *Chem. Commun.* 1407 (**1998**).
34. A. M. Liu, K. Hidajat, S. Kawi, and D. Y. Zhao, *Chem. Commun.* 1145 (**2000**).
35. R. Anwander, C. Palm, G. Gerstberger, O. Groeger, and G. Engelhard, *Chem. Commun.* 1811 (**1998**).
36. M. L Guzman-Castillo, H. Armendariz-Herrera, A. Tobon-Cervantes, D. R. Acosta, P. Salas-Castiilo, A. Montoya de la, F. A. Vazquez-Rodriguez, R. Alello, G. Giordano, F. Testa (eds.), *Stud. Surf. Sci. Catal.* 142, 1039 (**2002**).
37. C.-L. Chen, S. Cheng, H.-P. Lin, S.-T. Wong, and C.-Y. Mou, *Appl. Catal. A: General.* 215, 21 (**2001**).
38. K. Nowinska, R. Formaniak, W. Kaleta, and A. Wacław, *Appl. Catal. A: General* 256, 115 (**2003**).
39. W. Kaleta, and K. Nowińska, *Chem. Commun.* 535 (**2001**).

40. A. Vinu, K. Shanmugapriya, G. Chandrasekar, V. Murugesan, and K. Ariga, *J. Nanosci. Nanotechnol.* 5, 542 **(2005)**.

41. P. Srinivasu, S. Alam, V. V. Balasubramanian, S. Velmathi, D. P. Sawant, W. Böhlmann, S. P. Mirajkar, K. Ariga, S. B. Halligudi, and A. Vinu, *Adv. Funct. Mater.* 18, 640 **(2008)**.

42. V. V. Balasubramanian, C. Anand, R. R. Pal, T. Mori, W. Böhlmann, K. Ariga, A. K. Tyagi, and A. Vinu, *Microporous Mesoporous Mater.* 121, 18 **(2009)**.

43. R. Logudurai, C. Anand, V. V. Balasubramanian, K. Ariga, P. Srinivasu, and A. Vinu, *J. Nanosci. Nanotechnol.* 10, 329 **(2010)**.

44. R. Mokaya, W. Jones, Z. Luan, M. D. Alba, and Klinowski, *J. Catal. Lett.* 37, 113 **(1996)**.

45. R. Schmidt, D. Akporiaye, M. Stocker, and O. H. Ellestad, *J. Chem. Soc. Chem. Commun.* 1493 **(1994)**.

46. W. Zhang, M. Froba, J. Wang, P. T. Tanev, J. Wong, and T. J. Pinnavaia, *J. Am. Chem. Soc.* 118, 9164 **(1996)**.

47. P. Wu and M. Iwamoto, *J. Chem. Soc. Faraday Trans.* 94, 2871 **(1998)**.

48. H. Kosslick, H. Landmesser, and R. Frecke, *J. Chem. Soc. Faraday Trans.* 93, 1849 **(1997)**.

49. N. S. Nesterenko, O. A. Ponomoreva, V. V. Yuschenko, I. I. Ivanova, F. Testa, F. Di Renzo, and F. Fajula, *Appl. Catal. A: General* 254, 261 **(2003)**.

50. S. Udayakumar, S. Ajaikumar, and A. Pandurangan, *Appl. Catal. A: Geneneral.* 307, 245 **(2006)**.

51. G. Du, Y. Yang, W. Qiu, S. Lim, and G. L. Haller, *Appl. Catal. A: Geneneral* 313, 1 **(2006)**.

52. Y.-Y. Huang, B.-Y. Zhao, and Y.-C. Xie, *Appl. Catal. A: General* 172, 327 **(1998)**.

53. M. Chidambaram, C. Venkatesan, and A. P. Singh, *Appl. Catal. A: General* 310, 79 **(2006)**.

54. S. Albertazzi, E. Rodriguez-Castellon, M. Livi, A. Jimenez-Lopez, and A. Vaccari, *J. Catal.* 228, 218 **(2004)**.

55. M. L. Occelli, S. Biz, and A. Auroux, *Appl. Catal. A: General* 183, 231 **(1999)**.

56. K. Chaudhari, R. Bal, T. Kr. Das, A. Chandwadkar, D. Srinivas, and S. Sivasanker, *J. Phys. Chem. B.* 104, 11066 **(2000)**.

57. E. Rodriguez-Castellon, A. Jimenez-Lopez, P. Maireles-Torres, D. J. Jones, J. Roziere, M. Trombetta, G. Busca, M. Lenarda, and L. Storaro, *J. Solid State Chem.* 175, 159 **(2003)**.

58. X. X. Wang, L. Veyre, F. Lefebvre, J. Patarin, and J. M. Basset, *Microporous Mesoporous Mater.* 66, 169 **(2003)**.

59. A. Tarafdar, A. B. Panda, and P. Pramanik, *Microporous Mesoporous Mater.* 84, 223 **(2005)**.

60. P. Salas, L. F. Chen, J. A. Wang, H. Armendariz, M. L. Guzman, J. A. Montoya, and D. R. Acosta, *Appl. Surf. Sci.* 252, 1123 **(2005)**.

61. M. Scheithauer, R. E. Jentoft, B. C. Gates, and H. Knozinger, *J. Catal.* 191, 271 **(2000)**.

62. A. Corma, J. M. Serra, and A. Chica, *Catal. Today.* 81, 495 **(2003)**.

63. L. F. Chen, L. E. Noren, J. A. Wang, X. L. Zhou, J. Navarrete, I. Hernandez, A. Montoya, P. Perez Romo, P. Salas, and S. C. Pergher, *Catalysis Today* 133–135, 331 **(2008)**.

64. S. R. Zhai, Z. P. Wei, Q. D. An, D. Wu, and Y. H. Sun, *J. Chinese. Chem. Soc.* 58, 181 **(2011)**.

65. L. F. Chen, J. A. Wang, L. E. Norena, J. Aguilar, J. Navarrete, P. Salas, J. A. Montoya, and P. Del Angel, *J. Solid State Chem.* 180, 2958 **(2007)**.

66. H. Kosslick, H. Landmesser, and R. Frecke, *J. Chem. Soc. Faraday Trans.* 93, 1849 **(1997)**.

67. H. G. Karge, G. Ohlmann, H. Pfeifer, and R. Fricke, (eds.), Studies in Surface Science and Catalysis, Elsevier, Amsterdam **(1991)**, Vols. 65, 133.

68. B. Thomas and S. Sugunan, *Microporous Mesoporous Mater.* 96, 55 **(2006)**.

69. F. Lonyi and J. Valyon, *Micro. Meso. Mater.* 47, 293 **(2001)**.

70. A. Corma, *Micropor. Mesopor. Mater.* 4, 249 **(1997)**.

71. A. Sakthivel and P. Selvam, *Catal. Lett.* 84, 37 **(2002)**.

72. T. Ushikubo and K. Wada, *J. Catal.* 148, 138 **(1994)**.

73. D. Shouro, Y. Moriya, T. Nakajima, and S. Mishima, *Appl. Catal. A.* 198, 275 **(2000)**.

74. D. Mao, G. Lu, and Q. Chen, *Appl. Catal A: General* 263, 83 **(2004)**.

75. K. Chaudhari, R. Bal, A. J. Chandwadkar, and S. Sivasanker, *J. Mol. Catal A: Chemical* 177, 247 **(2002)**.

76. D. P. Serrano, J. Aguado, and J. M. Escola, *Ind. Eng. Chem. Res.* 39, 1177 **(2000)**.

Received: 28 February 2013. Accepted: 7 May 2013.